Available online at www.sciencedirect.com
SCIENCE DIRECT
Forest Ecology and Management 183 (2003) 313–325
Forest Ecology and Management
www.elsevier.com/locate/foreco

Radial-growth forecasts for five high-elevation conifer species on Vancouver Island, British Columbia

Colin P. Laroque, Dan J. Smith*
University of Victoria Tree-Ring Laboratory, Department of Geography, University of Victoria, Victoria, BC, Canada V8W 3P5

Received 22 November 2002; received in revised form 22 January 2003; accepted 22 February 2003

Abstract

Biologically-based deterministic multiple regression models are developed to investigate the consequences of future climates on the radial-growth response of five high-elevation conifer species on Vancouver Island. Historical climate data and tree-ring chronologies are used to establish robust relationships between climate and radial growth. Coupled general circulation modeled (CGCM) outputs are then used to provide monthly predictions of future climates from 2000 to 2100 A.D. The established historical relationships are projected into the future using the CGCM data to predict radial growth. Results indicate that each species will react individually to predicted changes in climate, with no one dominant radial-growth trend established. The most radical changes in the radial-growth behavior occur within mountain hemlock (*Tsuga mertensiana*) trees that have adapted to survive in deep snowpack environments, a condition that future predictions highlight as the most susceptible to change.

Keywords: Coupled general circulation model; High-elevation conifer species; Radial-growth forecasts

1. Introduction

Climates on the southwest coast of British Columbia have varied widely over the past 10,000 (Hebda, 1995), 1000 (Laroque, 1995; Zhang, 1996) and even 100 years (Heikkinen, 1984; Vincent, 1998; Mekis and Hogg, 1999; Vincent and Gullett, 1999). Since the end of the Little Ice Age in the 1850s to 1860s, warming climates have resulted in an unprecedented period of enhanced radial growth throughout this region (Innes, 1991; McKenzie et al., 2001; Lewis, 2001). While there is no simple explanation for this growth behavior (Laroque and Smith, 1999; Zhang, 2000; Gedalof and Smith, 2001), the influence of growing season temperature increases (Heikkinen, 1985; Luckman et al., 1997) and elevated CO_2 levels are suspected causal influences (Graumlich, 1991; McConnaughay et al., 1996).

Forecasting the radial-growth response of trees in this region to future climate changes is problematic, as most existing predictions are based upon a simple linear trend analyses of radial growth (e.g. McKenzie et al., 2001) from past to present rates using a variety of standardization techniques (Innes, 1991). Unfortunately this approach fails to account for the varied climate–growth response of individual tree species that is related to their natural ecological amplitude and differing ecological thresholds. Instead, there is broad agreement that robust forecast models must take

* Corresponding author. Tel.: +1-250-721-7328; fax: +1-250-721-6216.
E-mail addresses: colin@uvtrl.geog.uvic.ca (C.P. Laroque), smith@uvic.ca (D.J. Smith).

0378-1127/$ – see front matter
doi:10.1016/S0378-1127(03)00110-5

into account the influence of these biological controls on tree growth if better forecast models are to be developed (Visser and Molenaar, 1992; McKenzie et al., 2001).

This paper investigates the consequences of predicted future climates on the radial-growth response of five different high-elevation tree species on Vancouver Island using a biologically based, deterministic model. In this instance, derived biological growth models are used to approximate the future radial growth of trees using temperature and precipitation forecasts derived from the Canadian Climate Center's second-generation coupled general circulation model (CGCM2). The radial-growth data used to elucidate the principle biological controls of tree growth comes from a tree-ring network that includes 40 sites and 88 tree-ring chronologies (Laroque, 2002).

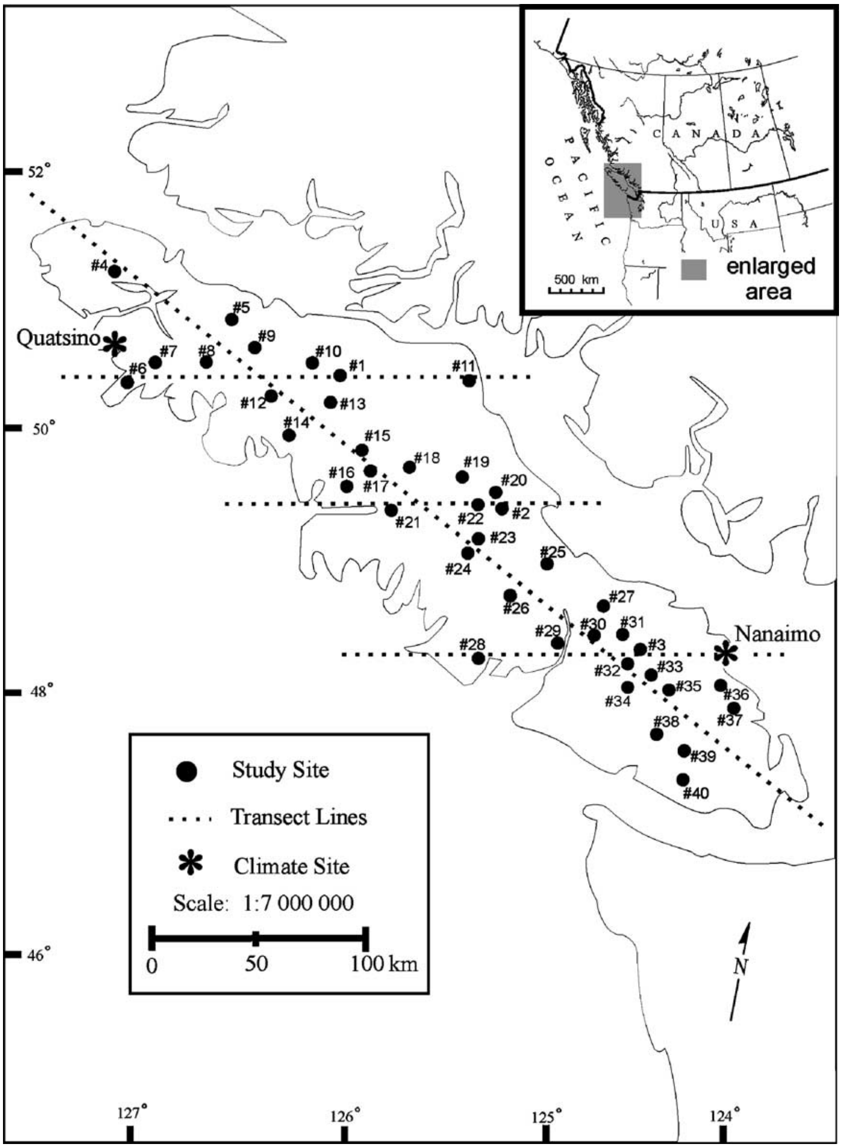

Fig. 1. Location of the 40 study sites on Vancouver Island, British Columbia, Canada.

2. Study sites and species

Vancouver Island, located on the west coast of British Columbia, Canada (Fig. 1), is positioned between 47 and 52° north latitude, 123 and 128° west longitude. The island has a northwest–southeast orientation, and is 450 km long and 75 km wide. Elevation varies from sea level to a maximum of 2200 m asl in the Vancouver Island Insular Mountain Range. These mountains run the length of Vancouver Island and modify the large-scale climatic forcing mechanisms that play a role in the island's biogeography (cf. Tuller, 1996).

Tree-ring samples were collected in the summers of 1996 and 1997 at 40 high-elevation sites in the mountain hemlock zone (MHZ) on Vancouver Island (Fig. 1). The MHZ is typified by short, cool summers and cool winters with a deep snowpack (Klinka et al., 1991). On Vancouver Island the dominant tree species in the MHZ are mountain hemlock (*Tsuga mertensiana*) and yellow-cedar (*Chamaecyparis nootkatensis*), with very minor components of amabilis fir (*Abies amabilis*) or subalpine fir (*Abies lasiocarpa*). At the lower elevation extent of the MHZ, western red-cedar (*Thuja plicata*), Douglas-fir (*Pseudotsuga menziesii*) and western hemlock (*Tsuga heterophylla*) trees are also present. Most trees in the MHZ grow in open areas as individuals or as part of small tree islands (Laroque et al., 2000/2001), but they can also be found in well-established stands (Pojar et al., 1991).

Increment cores were collected from mature co-dominant trees at sites with similar topographic and stand characteristics (Table 1). Treeline areas were selected because strong climate signals are characteristically retained in the tree-ring records of trees growing at their tolerance limits (Fritts, 1976). Whenever possible, summit locations were chosen to reduce noise resulting from the ecological consequences of slope and aspect (Fonda and Bliss, 1969). When locations other than the summit had to be sampled, areas with as little slope as possible were sought.

The sites were located at equidistant positions along a northwest–southeast longitudinal transect and along three east–west latitudinal transects. Sites along the east–west transects were selected to identify any wet-side/dry-side effects that might be present along the length of Vancouver Island. Where possible, sampling took place at locations above 1000 m asl elevation and at the local upper-elevation limit of growth for each tree species. At most sites the upper extent of yellow-cedar growth was found between 1250 and 1300 m asl and for mountain hemlock was limited to sites found below 1300–1500 m asl.

Sampling protocols followed two strategies. In the case of mountain hemlock and yellow-cedar trees, increment core sampling was restricted to trees found within open subalpine tree islands. Previous research on Vancouver Island has shown that sampling at this type of site greatly diminishes the problems attendant with competition in closed stands (Laroque, 1995; Smith and Laroque, 1996, 1998a,b; Laroque and Smith, 1999). In the case western hemlock, western red-cedar and Douglas-fir trees, increment core sampling was preferentially conducted within open stands but, in a few instances, did necessarily occur under a continuous canopy.

3. Methods

3.1. Tree-ring data

The crossdated chronologies were analyzed to see if any spatial patterns existed. An 88×88 chronology correlation matrix was constructed to compare these relationships over a common time frame from 1793 to 1993, a well-replicated 200-year interval in all of the chronologies (Laroque, 2002). Most within-species cross correlations were highly significant ($P < 0.0001$), with very few site-to-site chronologies failing to show the same radial-growth trends. The strongest correlations were usually from nearby sites of the same species. Between-species tests often showed a high correlation, especially when the two chronologies came from the same or nearby locations. The strongest correlations between species pairs were for mountain hemlock and western hemlock, and between mountain hemlock and yellow-cedar.

To reveal any north-to-south variation in these growth relationships, six sites from northern Vancouver Island were compared to six sites from southern Vancouver Island containing both a mountain hemlock and a yellow-cedar chronology (Table 2). In general, there was a very strong similarity within each species group, with all the northern and southern chronologies indicating significance above the $P < 0.0001$ level.

This spatial consistency and temporal stability suggests that if an outside climate regulator does affect annual radial-growth trends on Vancouver Island, that all the trees of a given species found at high-elevation sites are similarly impacted. These broad-scale island-wide associations present an opportunity to compile the 88 chronologies into five averaged, species-specific master chronologies (Fig. 2).

Table 1
The 40 study sites and sampling information

No.	Name	Tree species sampled					Site description (latitude, longitude, average elevation, NTS map sheet, UTM coordinate)
		MH	YC	WH	DF	WRC	
1	Mount Cain	x	x	x			50°13′55″N, 126°19′30″W, 1100 m asl, 92 L/1, 907670
2	Mount Becher	x	x				49°39′30″N, 125°12′40″W, 1120 m asl, 92 F/11, 407023
3	Green Mountain	x	x	x			49°03′20″N, 124°20′25″W, 1200 m asl, 92 F/1, 021344
4	Mount MacIntosh	x	x				50°40′10″N, 127°51′20″W, 696 m asl, 92 L/12, 808133
5	Castle Mountain	x	x				50°28′10″N, 127°03′00″W, 1100 m asl, 92 L/1, 907670
6	Butterfly/Wolf Ridge	x	x				50°11′10″N, 127°43′05″W, 610 m asl, 92 L/4, 899595 50°11′00″N, 127°44′20″W, 518 m asl, 92 L/4, 916603
7	Colonial Creek	x	x				50°17′30″N, 127°33′20″W, 915 m asl, 92 L/5, 031722
8	Bulldog Ridge	x	x				50°17′50″N, 127°14′00″W, 870 m asl, 92 L/6, 259731
9	Mrs. Wade Mountain	x	x				50°21′30″N, 126°53′05″W, 1097 m asl, 92 L/7, 503804
10	Mount Elliot	x	x				50°17′50″N, 126°29′55″W, 1433 m asl, 92 L/8, 780744
11	Mount Menzies	x	x				50°12′15″N, 125°28′10″W, 915 m asl, 92 K/3, 232643
12	Apple Tree Hill	x	x				50°08′00″N, 126°46′55″W, 1036 m asl, 92 L/2, 582550
13	Maquilla Peak	x	x				50°07′55″N, 126°21′45″W, 1220 m asl, 92 L/1, 891563
14	Silver Spoon Saddle	x	x				49°58′30″N, 126°40′45″W, 900 m asl, 92 E/15, 664386
15	South Sheena Creek	x	x				49°55′45″N, 126°09′55″W, 1158 m asl, 92 E/16, 032348
16	Nesook Creek		x	x		x	49°46′45″N, 126°16′50″W, 610 m asl, 92 E/16, 964166
17	Mount Upana	x	x				49°49′10″N, 126°07′20″W, 1025 m asl, 92 E/16, 073225
18	Mount Heber	x	x				49°53′50″N, 125°55′50″W, 1375 m asl, 92 F/13, 89831
19	Lupine Mountain	x	x				49°49′15″N, 125°31′00″W, 1300 m asl, 92 F/13, 189215
20	Mount Washington	x	x				49°44′35″N, 125°17′30″W, 1400 m asl, 92 F/11, 350130
21	Hanging Valley Creek	x	x				49°40′10″N, 125°58′30″W, 1130 m asl, 92 F/12, 855061
22	Circlet Lake	x					49°41′30″N, 125°23′30″W, 1260 m asl, 92 F/11, 280070
23	Milla Lake	x	x				49°33′20″N, 125°23′00″W, 1380 m asl, 92 F/11, 265924
24	Cream Lake	x					49°29′00″N, 125°31′00″W, 1280 m asl, 92 F/5, 166846
25	Mount Apps	x	x				49°26′30″N, 124°57′55″W, 1200 m asl, 92 F/7, 578779
26	Mount Porter	x	x				49°18′30″N, 125°13′45″W, 1140 m asl, 92 F/6, 380645
27	Mount Arrowsmith	x	x	x			49°16′15″N, 124°37′30″W, 1120 m asl, 92 F/7, 818585
28	Mount Redford		x	x		x	49°01′30″N, 125°24′40″W, 680 m asl, 92 F/3, 239333
29	Pirate Peak	x	x				49°06′20″N, 124°52′55″W, 1010 m asl, 92 F/2, 625407
30	Douglas Peak	x	x				49°08′10″N, 124°38′45″W, 1365m asl, 92 F/2, 802432
31	Mount Moriarty	x	x	x			49°08′30″N, 124°28′00″W, 1400 m asl, 92 F/1, 932440
32	Wapiti Ridge	x	x	x			48°59′40″N, 124°26′20″W, 1040 m asl, 92 C/16, 948277
33	Haley Lake	x		x			49°00′30″N, 124°18′45″W, 1320 m asl, 92 F/1, 043293
34	Heather Mountain	x	x				48°57′37″N, 124°27′23″W, 1135 m asl, 92 C/16, 936232
35	Mount Franklyn	x			x		48°54′40″N, 124°11′00″W, 1060 m asl, 92 C/16, 118163
36	Mount Brenton	x	x				48°54′00″N, 123°50′50″W, 1305 m asl, 92 B/13, 380166
37	Mount Prevost				x		48°49′50″N, 123°43′50″W, 780 m asl, 92 B/13, 441089
38	T–A–D Ridge	x	x	x			48°41′40″N, 124°16′40″W, 980 m asl, 92 C/9, 062941
39	Mount Modeste	x	x	x			48°38′20″N, 124°06′20″W, 1100 m asl, 92 C/9, 183875
40	San Juan Ridge	x	x	x			48°31′15″N, 124°07′50″W, 1000 m asl, 92 C/9, 163748

Tree species sampled are abbreviated as follows: MH, mountain hemlock; YC, yellow-cedar; WH, western hemlock; DF, Douglas-fir; WRC, western red-cedar.

Table 2
A correlation matrix of a 200-year time series of radial-growth increments from within and between groups at the six most northern and six most southern study sites on Vancouver Island

Name	Green Mountain	Heather Mountain	Wapiti Ridge	T–A–D Ridge	Mount Modeste	San Juan Ridge	Bulldog Ridge	Castle Mountain	Mrs. Wade Mountain	Mount Elliot	Apple Tree Hill	Mount Maquilla
Green Mountain	–	**0.52**	**0.5**	**0.35**	**0.44**	**0.36**	**0.39**	**0.46**	**0.38**	**0.62**	**0.28**	**0.49**
Heather Mountain	0.72	–	**0.36**	**0.22 (0.005)**	**0.3**	**0.33**	**0.35**	**0.4**	**0.29**	**0.41**	**0.27**	**0.19 (0.006)**
Wapiti Ridge	0.36	0.42	–	**0.7**	**0.5**	**0.22 (0.005)**	**0.52**	**0.42**	**0.52**	**0.27**	**0.21 (0.003)**	**0.37**
T–A–D Ridge	0.42	0.44	0.47	–	**0.52**	**0.27**	**0.52**	**0.38**	**0.29**	**0.14 (0.04)**	**0.22 (0.002)**	**0.42**
Mount Modeste	0.63	0.74	0.38	0.64	–	**0.58**	**0.61**	**0.57**	**0.5**	**0.41**	**0.58**	**0.49**
San Juan Ridge	0.45	0.65	0.43	0.53	0.67	–	**0.37**	**0.48**	**0.37**	**0.57**	**0.73**	**0.32**
Bulldog Ridge	0.38	0.47	0.06 (0.385)	0.41	0.66	0.45	–	**0.55**	**0.26**	**0.36**	**0.39**	**0.58**
Castle Mountain	0.5	0.57	0.28	0.55	0.7	0.49	0.67	–	**0.56**	**0.56**	**0.52**	**0.51**
Mrs. Wade Mountain	0.48	0.51	0.34	0.57	0.57	0.52	0.49	0.70	–	**0.57**	**0.66**	**0.36**
Mount Elliot	0.46	0.61	0.33	0.48	0.68	0.52	0.52	0.52	0.56	–	**0.51**	**0.31**
Apple Tree Hill	0.39	0.5	0.19 (0.008)	0.41	0.68	0.59	0.85	0.64	0.56	0.57	–	**0.42**
Mount Maquilla	0.31	0.49	0.23 (0.001)	0.35	0.61	0.51	0.56	0.48	0.44	0.59	0.54	–

Mountain hemlock correlations are in bold, while yellow-cedar correlations are not in bold. Values of Pearson's *r* are listed with *P*-values in brackets when the correlation results are below the 0.0001 level.

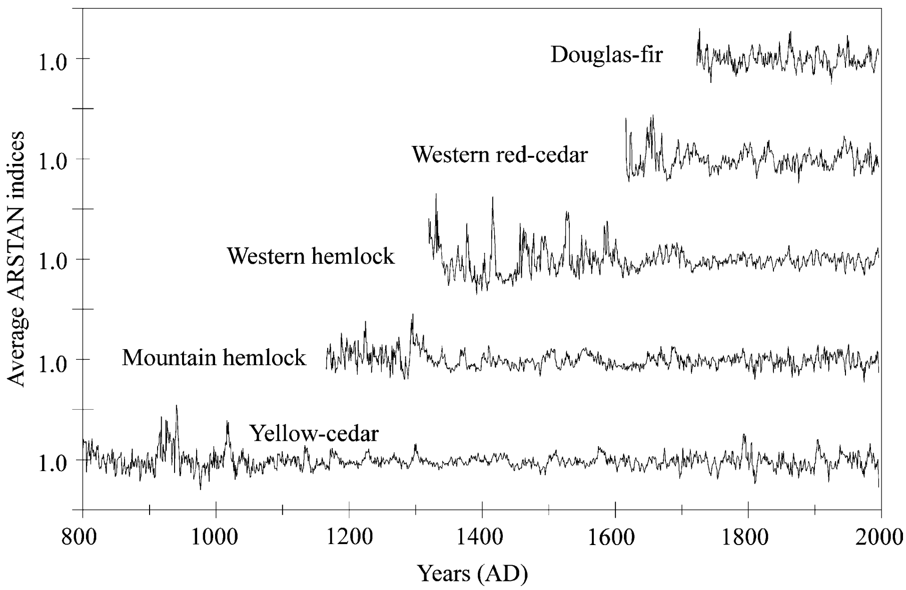

Fig. 2. The five master chronologies averaged from the 88 chronologies that made up the sampling network in the study.

3.2. Past climate data

Regression models were developed for each tree species to establish mathematical relationships between radial growth and climate, by comparison with long-term monthly climate data from the Nanaimo station from 1900 to 1995 ($n = 95$). Forty temperature and precipitation variables for 20 months from the previous year's May to the end of the current year were selected for comparison to the averaged annual ring-width parameter. A 1-year prior growth value was added as an independent variable, as high autocorrelation values and previous research strongly suggest that the radial growth in the previous year has a large bearing on radial increments in the growth year (Laroque, 1995, 2002; Smith and Laroque, 1996, 1998a; Gedalof and Smith, 2001).

The most significant independent variables (40 climate and one lag variable) influencing the radial growth of each tree species were selected by first entering all the variables into a forward stepwise multiple regression. This procedure steps each variable into a regression equation and sequentially distinguished those having the largest partial correlation on the overall equation. In this manner the independent variables that had the least amount of consequence to the regression equation can easily be highlighted and eliminated. Subsequently, the significant variables were re-entered into a data-limited stepwise multiple regression equation. The "*F* to enter" and "*F* to remove" confidence levels were set at 0.10 and 0.15, respectively, to limit the number of independent variables entered into each equation and to approximate a "10%" rule of thumb. Given 95 years of data from the Nanaimo station, the inclusion of from 7 to 13 independent variables ensured that 'overfitting' of the regression equation did not occur (Sokal and Rohlf, 1997) (Table 3).

These climate–growth analyses show that from 55 to 68% of the annual variance in radial growth in the five high-elevation tree species can be explained using climate data from Nanaimo (Table 3). All the models were found to be highly significant when verified using standard goodness-of-fit tests.

3.3. Future climate data

The climatic character of Vancouver Island over the next century was modeled using forecasts generated by the Canadian Climate Centre second-generation CGCM2 (http://www.cccma.bc.ec.gc.ca/eng_index.html, accessed 16 November 2001). The CGCM2 couples the second-generation atmospheric general circulation model (AGCM2) (McFarlane et al., 1992) with an ocean component (a modular ocean module and a

Table 3
Results of a stepwise multiple regression analysis between radial growth and climate data from Nanaimo station (1900–1995) and the CGCM2 data from a regional grid square (1900–1995)

Dependent variable (model)	Number of independent variables in the equation	Explained r (r^2) (actual data)	Explained r (r^2) (GCM2 data)
Master mountain hemlock	12	0.78 (0.60)	0.68 (0.46)
Master yellow-cedar	8	0.78 (0.60)	0.67 (0.46)
Master western hemlock	8	0.81 (0.66)	0.71 (0.50)
Master western red-cedar	13	0.82 (0.68)	0.67 (0.45)
Master Douglas-fir	7	0.74 (0.55)	0.63 (0.40)

All models include a 1-year lag parameter and are significant at $P < 0.0001$.

sea ice model) to better model ocean–atmosphere interactions (Flato et al., 2000; Flato and Boer, 2001). CO_2 forcing in the CGCM2 model is derived from the measured rates of change from 1900 to 1996 and is calculated as an annual 1% increase in CO_2 for the remaining years (Flato et al., 2000). For this application, the CGCM2 outputs from a 3.75° × 3.75° GCM grid centered over 50°10′N latitude, 127°50′W longitude were employed to forecast future radial growth. The grid encompasses the northern two-thirds of Vancouver Island, a section of the British Columbia Coast Mountains and a portion of the nearby Pacific Ocean.

CGCM2 is intended to provide climate predictions for the period 1900 to 2100 A.D. In this instance, precipitation was summed as monthly totals and the temperature data were reported as monthly means in degrees centigrade. To test the capacity of CGCM2 for modeling Vancouver Island climates, the model outputs were compared to two long-term records of climate (Nanaimo and Quatsino) for the period 1900–2000. A comparison of the actual to predicted climates shows that CGCM2 generated temperature predictions were consistently 2–3 °C cooler than those recorded at either Nanaimo or Quatsino in the summer months, but were consistently warmer than the

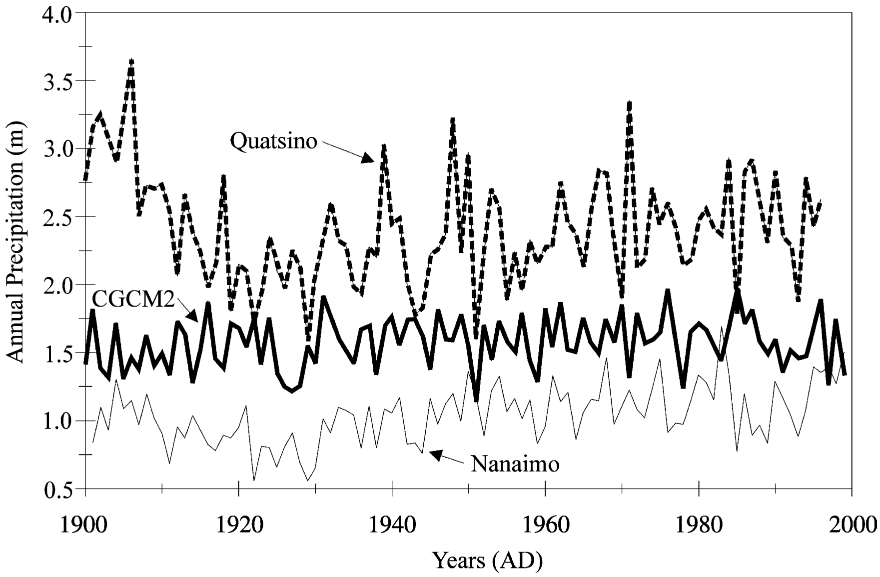

Fig. 3. A comparison of precipitation data from Nanaimo and Quatsino on Vancouver Island (1900–2000), and the CGCM2 data derived from the surrounding grid square.

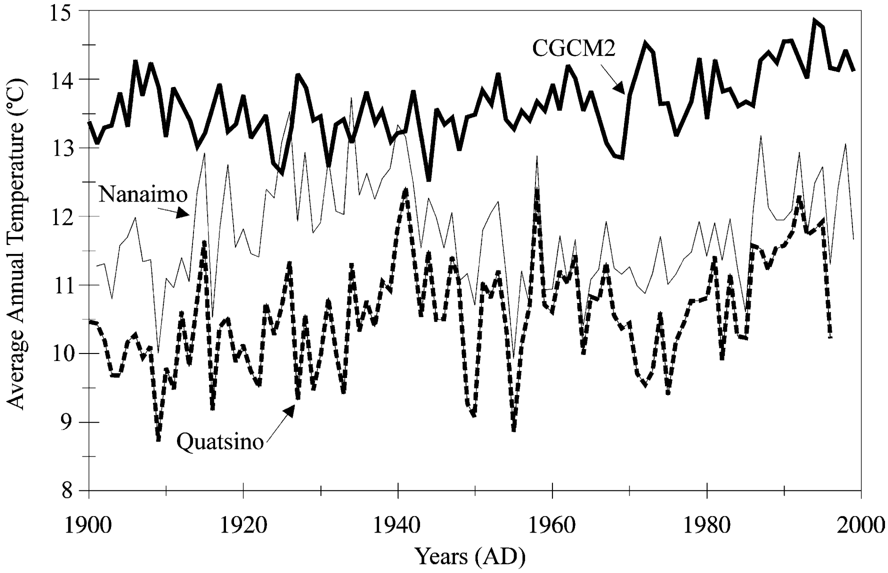

Fig. 4. A comparison of temperature data from Nanaimo and Quatsino on Vancouver Island (1900–2000), and the CGCM2 data derived from the surrounding grid square.

recorded temperatures for the remainder of the year (Fig. 4). Similarly, the CGCM2 precipitation predictions were consistently greater than those recorded at Nanaimo, but consistently below those recorded at Quatsino (Figs. 3 and 4). These characteristics are assumed a consequence of differences between the oceanic character of the GCM grid and precipitation trends at the two stations. The windward location of Quatsino, on the western slopes of the Insular Mountains, leads to exaggerated orographic precipitation and the leeward, rainshadow location of Nanamio limits the annual precipitation totals.

Despite the inability of the CGCM2 outputs to exactly match individual station records over the last century, there is sufficient similarity between the actual and predicted climate data to suggest that the climate forecasts generated for 2000–2100 A.D. are indicative of forthcoming trends on Vancouver Island. These forecasts suggest that this region should expect an increase in the annual precipitation total of ca. 20 cm, but that the year-to-year variability will be similar to that experienced over the last century (Fig. 5A). By contrast, CGCM2 indicates that the average annual temperature in this region will increase by ca. 4 °C, rising from an average of 14.5 °C in 2000 to 18.5 °C by 2100 (Fig. 5B).

3.4. Forecasting radial growth

The climate–radial-growth relationships established previously by stepwise regression analysis were re-examined using the CGCM2 models of climate between 1900 and 2000 A.D. As Table 3 illustrates, the explanatory ability of the CGCM2 climate data to describe the annual radial-growth tends decreases from 55–68 to 40–50%. Despite these losses, goodness-of-fit tests indicate that the CGCM2 forecasts still offer a robust perspective of the role that climate played on the annual radial-growth trends over the last century. This new relationship is used to indicate the radial growth of the five tree species under study, by predicting their response to climate changes forecasted by CGCM2 forecasts until 2100.

4. Results

The radial-growth response of mountain hemlock trees on Vancouver Island to past (1990–1995) and future (1995–2100) climates is shown in Fig. 6A. Over this time frame, the radial growth of mountain hemlock trees varies within its long-term range of variation until 2030, when a sharp decline in ring growth is

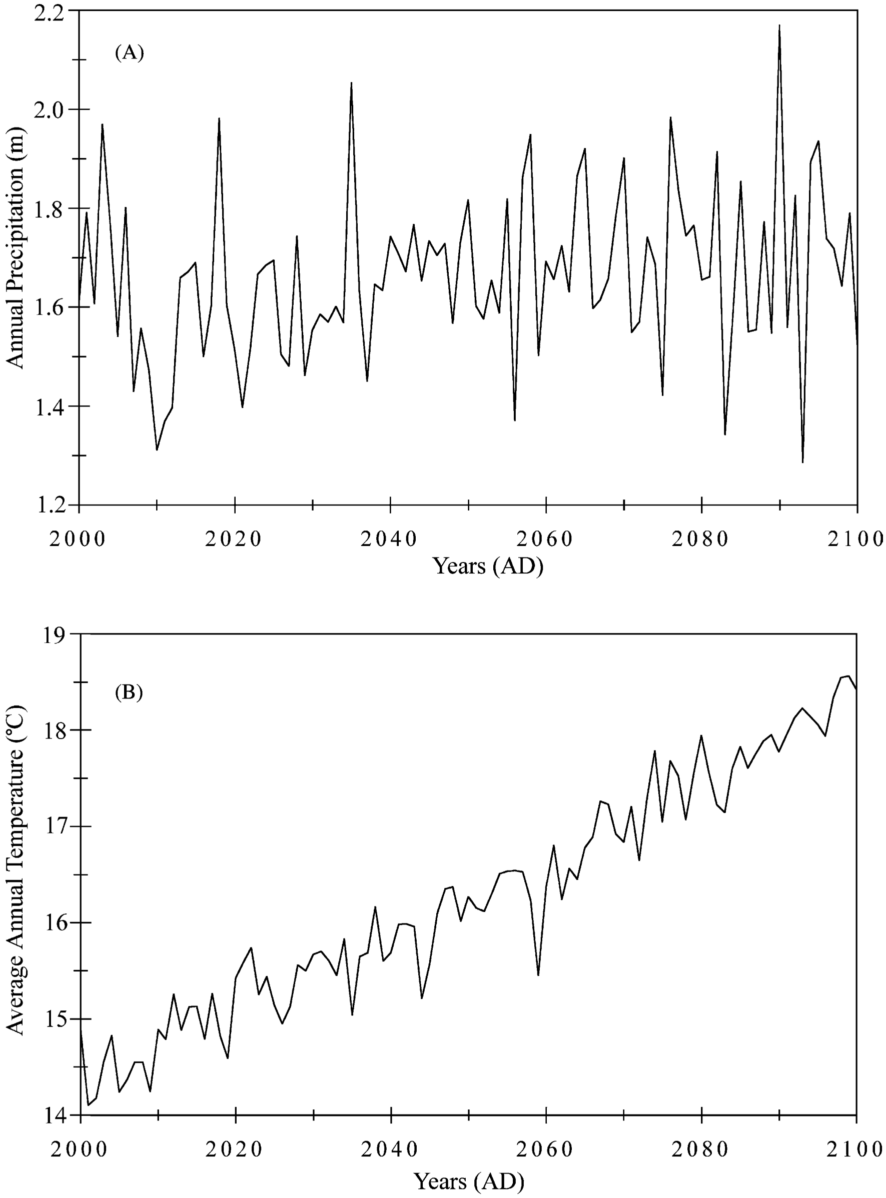

Fig. 5. Future predicted CGCM2 data from 2000 to 2100 for the grid square surrounding Vancouver Island for (A) precipitation and (B) temperature.

inaugurated that, by the 2060s, exceeds the smallest recorded annual growth increments. Mountain hemlock radial growth continues to decline until the end of the forecast period. The response of mountain hemlock trees to future climates is similar to that displayed by western hemlock until ca. 2040 (Fig. 6B). Unlike the growth response of mountain hemlock after this time, western hemlock trees continue to add annual growth increments that fall within a range of variation that characterized tree-ring growth throughout the 20th century. By way of contrast, yellow-cedar and Douglas-fir continue to add annual growth increments similar in size to those recorded over the preceding century until the 2040s (Fig. 6C and D). After this

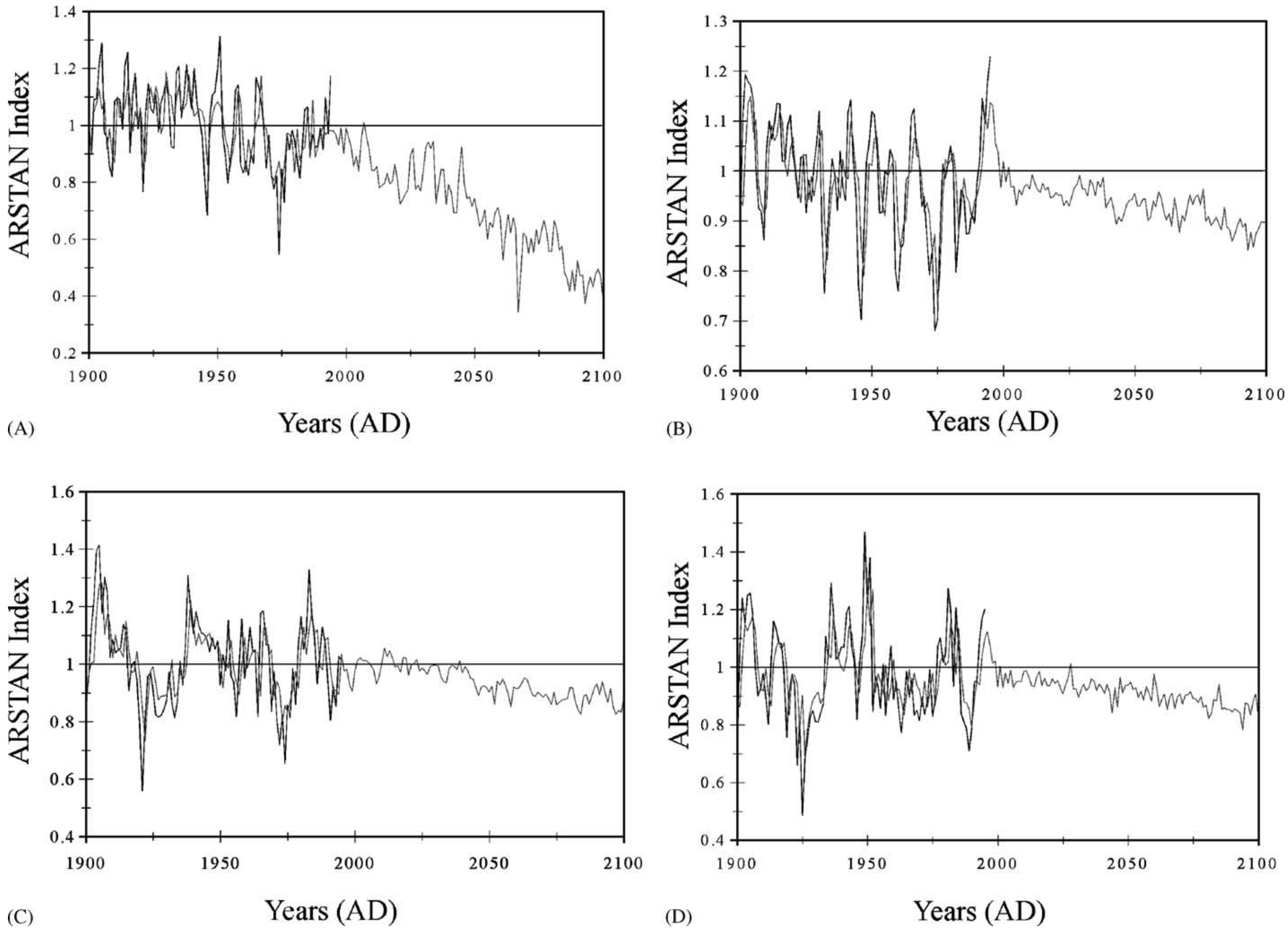

Fig. 6. Future predicted radial-growth trends for each of the five species in the study: (A) mountain hemlock; (B) western hemlock; (C) yellow-cedar; (D) Douglas-fir; (E) western red-cedar.

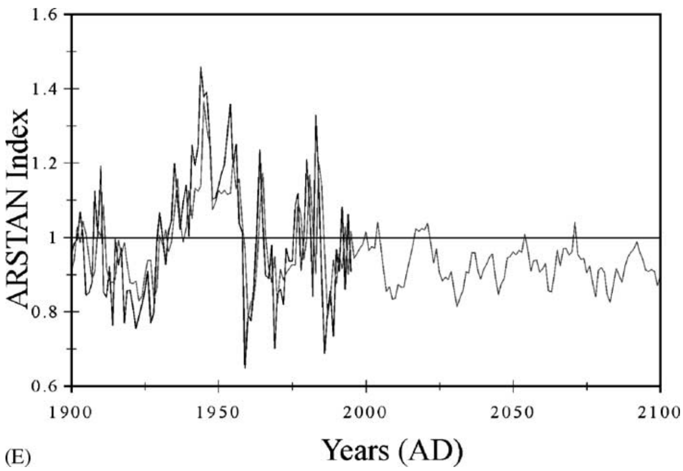

Fig. 6. (*Continued*).

point in time, radial growth remains at or near the low end of the long-term range of variation for both species.

The radial-growth response of high-elevation western red-cedar trees to future climates is the most complex of those examined (Fig. 6E). Western red-cedar exhibits a sudden increase in radial growth, followed by an equally sudden reduction in growth in the first 10 years of the new century. Radial growth slowly recovers throughout the 2010s and 2020s, until it regains a position slightly above the historical 20th century average. In the 2030s, the rate of western red-cedar radial growth again decreases, only to increase throughout the late 2050s and the 2060s. Western red-cedar radial growth maintains near average levels until 2100, where it has a below-average growth rate at the end of the forecast.

5. Discussion

The future climate–growth response of all five high-elevation tree species display an overall reduction in the year-to-year variability in productivity. While this trait might be indicative of more consistent environmental conditions at these sites, it is also likely related to the CGCM2 forecasts that were designed to deliver a homogenized interpretation of climates over of a large grid square. Furthermore, as only 7–13 climate factors were utilized within the predictive models, it may be that the influence of a host of other climatic and non-climatic factors becomes more limiting to growth as the climate continues to change.

The distinctive response of mountain hemlock trees to future climates may be related to the influence of changing springtime environments, when notable reductions in April–June precipitation totals are predicted by the CGCM2 forecasts. Previous analysis of the relationship between climate and radial growth on Vancouver Island mountain hemlock trees has emphasized the importance of precipitation during this period (Smith and Laroque, 1998a; Lewis and Smith, 1999; Gedalof and Smith, 2001). Particularly crucial to understanding this growth response would be an assessment of whether the forecasted precipitation will fall as snow or rain (cf. Peterson and Peterson, 2001), especially given that large spring snowpacks are known to limit mountain hemlock radial growth (Graumlich and Brubaker, 1986; Smith and Laroque, 1998a; Gedalof and Smith, 2001; Laroque, 2002).

Although greatly improved over past models, long-term deterministic forecast models like the one employed in our analysis cannot fully model the ecological amplitude or plasticity inherent in most trees (Zhang et al., 2000). For instance, in the case of mountain hemlock trees it remains to be seen if they have the ability to adapt to the predicted climate changes. While mountain hemlock trees growing at high-elevation in northern California have the ability to derive most of their moisture from winter precipitation to survive (Burns and Honkala, 1990), there is no evidence to suggest that more northerly populations that experience reduced photoperiods could make the same adjustments. If they cannot, lower elevational stands on Vancouver Island are liable to become increasingly senescent and may eventually die off. There is also some probability that the elevation extent of mountain hemlock trees may increase as more favorable conditions for germination become commonplace above the present treeline. Unfortunately, in the case of Vancouver Island, there is little higher terrain to move to. On the rest of the Pacific coast mountain hemlock could conceivably move up into elevations presently occupied by subalpine fir, if competitive interactions do not limit their upward migration.

6. Conclusion

Forecast models for radial growth of trees have never before been attempted with climate data. Long-term radial-growth models were developed using CGCM2 data from the Canadian Climate Centre. Regression analyses established climate–growth relationships for five master chronologies to the forecasted data. The strength of these relationships ranged from a low of 40% of the variance explained for Douglas-fir to a high of 50% for yellow-cedar. Forecasts were made from the data for the years 2000–2100 A.D.

Mountain hemlock was shown to be the tree species most susceptible to impact from the forecasted climate changes. While the radial growth of the other species examined were shown to experience slight reductions in radial growth over this interval, these were comparably minor and probably within a range of error when compared to the more dramatic potential impact on mountain hemlock populations. What cannot be modeled is the ability of the mountain hemlock species to adequately incorporate the warmer and drier spring conditions into its radial-growth increment. If the species can take advantage of more normal spring conditions occurring at an earlier calendar period, it may continue to flourish in its current Pacific northwest environments. If it cannot, then it may slowly be replaced in its current environment by other species that can, and it will also have to migrate to more favorable locations in the environment, or face being slowly eliminated.

Long-term forecasting as presented in this study is by no means highly certain, as it focuses only on the impacts generated by forecasted changes inherent within the Canadian climate model. Nevertheless, these predictions of future forest productivity break new ground in that they use actual forecasted data to predict radial growth instead of relying upon past trends to predict future radial growth. Despite any shortcomings of this application, it does provide a starting point for forest managers and forest ecologists to evaluate what effect future climates may have on tree growth.

Acknowledgements

The research presented in this paper was supported by grants from Forest Renewal British Columbia (FRBC); the Natural Sciences Engineering and Research Council (NSERC) and the University of Victoria awarded to Dan J. Smith. We gratefully acknowledge the reviewers for their improvements to the manuscript.

References

Burns, R.M., Honkala, B.H., 1990. Silvics of North America, Volume 1, Conifers. Forest Service Agriculture Handbook, USDA, Washington, DC, p. 654.

Flato, G.M., Boer, G.J., 2001. Warming asymmetry in climate change simulations. Geophys. Res. Lett. 28, 195–198.

Flato, G.M., Boer, G.J., Lee, W.G., McFarlane, N.A., Ramsden, D., Reader, M.C., Weaver, A.J., 2000. The Canadian centre for climate modelling and analysis global coupled model and its climate. Climate Dynamics 16, 451–467.

Fonda, R.W., Bliss, L.C., 1969. Forest vegetation of the montane and subalpine zones, Olympic Mountains, Washington. Ecol. Monogr. 39, 271–301.

Fritts, H.C., 1976. Tree Rings and Climate. Academic Press, London.

Gedalof, Z.M., Smith, D.J., 2001. Dendroclimatic response of mountain hemlock (*Tsuga mertensiana*) in Pacific North America. Can. J. Forest Res. 31, 322–332.

Graumlich, L.J., 1991. Subalpine tree growth, climate, and increasing CO_2: an assessment of recent growth trends. Ecology 72, 1–11.

Graumlich, L.J., Brubaker, L.B., 1986. Reconstruction of annual temperature (1590–1979) for Longmire, Washington, derived from tree rings. Quaternary Res. 25, 223–234.

Hebda, R.J., 1995. British Columbia vegetation and climate history with a focus on 6 KA BP. Géographie physique et Quaternaire 49, 55–79.

Heikkinen, O., 1984. Dendrochronological evidence of variations of Coleman Glacier, Mount Baker, Washington, USA. Arctic Alpine Res. 16, 53–64.

Heikkinen, O., 1985. Relationships between tree growth and climate in the subalpine Cascade Range of Washington, USA. Ann. Bot. Fennici 22, 1–14.

Innes, J.L., 1991. High-altitude and high-latitude tree growth in relation to past, present and future global climate change. The Holocene 1, 168–173.

Klinka, K., Pojar, J., Meidinger, D.V., 1991. Revision of biogeoclimatic units of coastal British Columbia. Northwest Sci. 65, 32–47.

Laroque, C.P., 1995. The dendrochronology and dendroclimatology of yellow-cedar on Vancouver Island, British Columbia. Unpublished M.Sc. thesis, University of Victoria, Victoria, BC, Canada.

Laroque, C.P., 2002. Dendroclimatic response of high-elevation conifers, Vancouver Island, British Columbia. Unpublished Ph.D. dissertation, University of Victoria, Victoria, BC, Canada.

Laroque, C.P., Smith, D.J., 1999. Tree-ring analysis of yellow-cedar (*Chamaecyparis nootkatensis*) on Vancouver Island, British Columbia. Can. J. Forest Res. 29, 115–123.

Laroque, C.P., Lewis, D.H., Smith, D.J., 2000/2001. Treeline dynamics on southern Vancouver Island, British Columbia. Western Geography 10–11, 43–63.

Lewis, D.H., 2001. Little Ice Age of Strathcona Provincial Park. Unpublished M.Sc. thesis, University of Victoria, Victoria, BC, Canada.

Lewis, D.H., Smith, D.J., 1999. Little Ice Age climate trends at treeline in Strathcona Provincial Park, Vancouver Island: insights from glaciers and trees. In: MacIver, D.C. (Ed.), Proceedings of the Workshop on Decoding Canada's Environmental Past: Adaptation Lessons Based on Changing Trends and Extremes in Climate Biodiversity. Atmospheric Environment Service, Downsview, pp. 19–29.

Luckman, B.H., Briffa, K.R., Jones, P.D., Schweingruber, F.H., 1997. Tree-ring based reconstruction of summer temperatures at the Columbia Icefield, Alberta, Canada, AD 1073-1983. The Holocene 7, 375–389.

McConnaughay, K.D.M., Nicotra, A.B., Bazzaz, F.A., 1996. Rooting volume, nutrient availability and CO_2-induced growth enhancement in temperate forest tree seedlings. Ecol. Appl. 6, 619–627.

McFarlane, N.A., Boer, G.J., Blanchet, J.P., Lazare, M., 1992. The Canadian climate centre second generation general circulation model and its equilibrium climate. J. Climate 5, 1013–1044.

McKenzie, D., Hessl, A.E., Peterson, D.L., 2001. Recent growth of conifer species of western North America: assessing spatial patterns of radial growth trends. Can. J. Forest Res. 31, 526–538.

Mekis, E., Hogg, W.D., 1999. Rehabilitation and analysis of Canadian daily precipitation time series. Atmosphere–Ocean 37, 53–85.

Peterson, D.W., Peterson, D.L., 2001. Mountain hemlock growth responds to climatic variability at annual and decadal time scales. Ecology 82, 3330–3345.

Pojar, J., Klinka, K., Demarchi, D.A., 1991. Mountain hemlock zone. In: Meidinger, D., Pojar, J. (Eds.), Ecosystems of British Columbia, British Columbia Ministry of Forests Special Report Series No. 6, Victoria, BC, Canada, pp. 113–124.

Smith, D.J., Laroque, C.P., 1996. Dendroglaciological dating of a little ice age glacial advance at Moving Glacier, Vancouver Island, British Columbia. Géographie physique et Quaternaire 50, 47–55.

Smith, D.J., Laroque, C.P., 1998a. Mountain hemlock growth dynamics on Vancouver Island. Northwest Sci. 72, 67–70.

Smith, D.J., Laroque, C.P., 1998b. High-elevation dendroclimatic records from Vancouver Island. In: MacIver, D.C., Meyer, R.E. (Eds.), Proceedings of the Workshop on Decoding Canada's Environmental Past: Climate Variations and Biodiversity Change during the Last Millennium. Atmospheric Environment Service, Downsview, pp. 33–44.

Sokal, R.R., Rohlf, F.J., 1997. Biometry: The Principles and Practice of Statistics in Biological Research. Freeman, New York.

Tuller, S., 1996. Climate. In: Wood, C.J.B. (Ed.), British Columbia, The Pacific Province: Geographical Essays. Canadian Western Geographical Series, vol. 36. Canadian Western Geographical Press, University of Victoria, Victoria, pp. 45–63.

Vincent, L.A., 1998. A technique for the identification of inhomogeneities in Canadian temperature series. J. Climate 5, 1094–1104.

Vincent, L.A., Gullett, D.W., 1999. Canadian historical and homogeneous temperature datasets for climate change analyses. Int. J. Climatol. 19, 1375–1388.

Visser, H., Molenaar, J., 1992. Estimating trends and stochastic response functions in dendroecology with an application to fir decline. Forest Sci. 38, 221–234.

Zhang, Q.B., 1996. A 2122-year tree-ring chronology of Douglas-fir and spring precipitation reconstruction at Heal Lake, southern Vancouver Island, British Columbia. Unpublished M.Sc. thesis, University of Victoria, Victoria, BC, Canada.

Zhang, Q.B., 2000. Modern and late holocene climate-tree-ring growth relationships and growth patterns in Douglas-fir, Coastal British Columbia, Canada. Unpublished Ph.D. dissertation, University of Victoria, Victoria, BC, Canada.

Zhang, Q.B., Hebda, R.J., Zhang, Q.J., Alfaro, R.I., 2000. Modeling tree-ring growth responses to climatic variables using artificial neural networks. Forest Sci. 46, 229–239.